A comparative study of ZnO, CuO and a binary mixture of $ZnO_{0.5}$-$CuO_{0.5}$ with nano-dye on the efficiency of the dye-sensitized solar cell

A comparative study of ZnO, CuO and a binary mixture of $ZnO_{0.5}$-$CuO_{0.5}$ with nano-dye on the efficiency of the dye-sensitized solar cell

Nibras Abdul-Ameer Aboud *[1]. Wafaa M.S Alkayat [2]. Dhia H Hussain[3], Ahmed Mahdi Rheima[4*]

[1]Department of Chemical Industrial, Institute of Technology/ Baghdad, Middle Technical University, Iraq.
[2]Physics Department, College of Science, Al-Mustansiriyah University, Baghdad, Iraq.
[3]Chemistry Department, College of Science, Al-Mustansiriyah University, Baghdad, Iraq.
[4]Chemistry Department, College of science, Wasit University, Kut, Iraq.

*Corresponding author: Email arahema@uowasit.edu.iq

Abstract

In this study, ZnO, CuO, and ZnO-CuO nanostructure with ZnO: CuO molar ratios of 1:1M, have been successfully synthesized via photolysis method. The synthesized nanostructure was designed to explore its morphology, structure and pureness. The XRD analysis confirmed that the synthesized particles are within the range of nanometers with their average particle size of below 100 nm, with SEM images showing the shape of the nanostructure. The purety of oxides was confirmed by the EDX analysis. Furthermore, the effect of adding nano dye on the performance of Dye sensitizes solar cells.Results showed that the added nano dye as A novel Nano copper complex as Bis [4-[(5-acetyl-2-aminophenyl) diazenyl] -1,5-dimethyl-2-phenyl-1H-pyrazole-3 (2H) -one] copper (II). In order to increase the surface grittiness of the active layer, hydrate improved absorption in the visible region. The power conversion efficiency (PCE), which was caused by an increase in Voc, Jsc and FF of the manufactured device, was improved through the inclusion of inorganic Dye.

Keywords: dye-sensitized Solar cell, photolysis, Nano dye, ZnO – CuO, structural properties.

Introduction

Energy is a significant need for the life and development of people. There is developing that solar cell energy will a doubt increasingly more significant in future energy-generating structure. Become Growing ease, high-productivity, and clean sunlight based vitality advancements will be critical long interests [1]. Solar cells can transform solar energy directly from one of the most convenient forms of energy in modern society to electricity. Solar cell application is cost-efficient, i.e. to achieve greater efficiency in energy conversion and less cost[2,3].

DSSCs is the most promising alternative to conventional solar cells, given the higher efficiency of photovoltaic conversion and reasonable price. In recent years, in addition to the problems of efficiency and stability of energy conversion, the vital issue is to reduce the cost of manufacturing emerging solar cells by introducing novel materials and technologies that depend on the development of nanomaterials and nanotechnology, in addition to using Semiconductor nanomaterials such as zinc and copper and titanium [4,5].

Semiconductor materials nanoparticles have gained more attention in recent years due to their desired properties and applications in different fields [6-13]. These nanomaterials are distinguished by the new electronic, structural, and thermal properties of great scientific importance in the primary and applied fields [14-18]. ZnO is a large-scale semiconductor with a power gap of 3.37 volts at room temperature. It has been widely used for its catalytic, electrical, photovoltaic and photochemical properties[19]
[20,21]. CuO nanostructures have a great advantage to apply to the process due to its large surface area. Since copper oxide displays different physical and chemical properties depending on the morphology of nanostructures, this is why it is considered one of the essential oxides for making solar cells [22,23]. In this project, ZnO, CuO, and ZnO-CuO nanostructure with ZnO: CuO molar ratios of 1:1M, have been synthesized by the photo-irradiation method Process and evaluate its efficiency for Dye sensitizes solar cells.

Experimental

Materials:

The materials were purchased and used by Sigma-Aldrich. The solvent was deionized water during the processing of oxide and purification procedures.

2.2. Synthesis of ZnO, CuO, and ZnO- Cu_2O nanostructure

The cell was used to irradiate the salt of zinc and copper, which were the source of ZnO, CuO, and ZnO-CuO nanostructure. UV source (mercury medium pressure lamps with power 125 watts). The UV lamps feature a wide range of UV and visible rays (200 nm to 600 nm) has maximum light intensity at the wavelength 365 nm,

1- 50 ml of 0.1M SHMP was used as a surfactant in the synthesis process, a stoichiometric ratio (1:2:5) (salt: base: SHMP) used so, 50 ml of 0.02 M Zn $(NO_3)_2$. $6H_2O$ was alternately mixed with SHMP drop by drop, and the mixture was stirred magnetically at 30°C until a homogeneous solution was obtained then, 25 ml of 0.04 M NaOH was added to the above solution. Irradiated by the photocell. A white precipitate of zinc (II) hydrate is obtained; wash the precipitate with a large amount of deionizing water, the precipitate is dried in an oven at 80°C for 2 h and calcined at 400°C for 3 hrs.

2- The stoichiometric ratio (1:2:5) (salt: base: SHMP) is used in preparation method, so 10 ml of 0.1 M SHMP added to 50 ml of (0.02 M) Cu $(NO_3)_2.3H_2O$ under continuous stirring at 30 ° C, 25 ml NaOH mixed with (salt-SHMP) solution, irradiated with a photocell for 30 minutes using cooling to 5 °C. The dark blue color precipitate obtained, the product was isolated, washed a several times with deionizing water and ethanol, separated by using a centrifuge for 20 min, The residuum has dried in an oven at 90°C for 2 hrs. Furthermore, Calcination at 250°C for 3 hrs. Dark black color precipitate has been obtained.

3- 50 ml of (0.02) M of Zn $(NO_3)_2.6H_2O$, in burette NaOH, was added dropwise to the zinc salt with (1: 2) (salt: base) a white suspension form (solution A),

50 ml of (0.02) M Cu $(NO_3)_2.3H_2O$ with (1: 2) (salt: base), 25 ml NaOH was added diagonally to the copper salt blue suspension form (solution B). Then solutions A and B were mixed to complete their radiant reaction with the photocell for 30 minutes using cooling at 5 °C to form dark blue deposits. The precipitate was washed with deionized water, centrifuged for 20 minutes, then dried at 90 ° C. Calcification at 500 ° C for 3 hrs. Brown precipitate has been observed.

2.3. Synthesis of A novel Nano copper complex as Bis[4-[(5-acetyl-2-aminophenyl)diazenyl]-1,5-dimethyl-2-phenyl-1H-pyrazol-3(2H)-one]copper(II).hydrate

Ligand de-ionized solution of (0.35 g, 0.1M) has been added with constant stirring at pH solution 7-9 prepared from ammonium acetate (771 mg, 10 Mm) in 1 L of de-ionized water. The pH (7-9) was adjusted using the NH_3 solution. To (0.08g, 0.05 M) $CuCl_2.2H_2O$ salt under ultrasonic sonication[17] for an hour and then be in a complex solution with Pale red color. The resulting suspension solution was washed several times with de-ionized water and let until the complex precipitate, then dried at room temperature. The suggested geometry, as shown in Scheme (1).

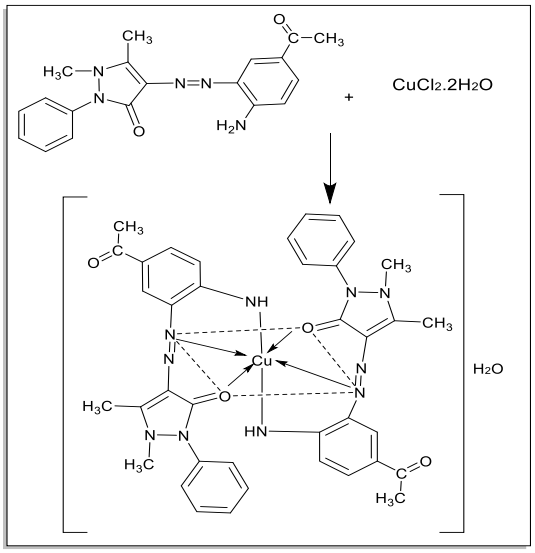

Scheme (1): Suggested geometry for Cu (II) complexes azo ligand.

2.4. Solar cell fabrication

1- Cathode electrode

The technique for vacuum evaporation is to heat until the material to be deposited has evaporated. The vapor eventually condenses into a thin layer on the aluminum substratum surface and the emptying chamber walls. In general, the contact between steam and atmosphere is prevented by low pressures around 10^{-6} or 10^{-5} Torr. At those low pressures, the average vapor atom free course is identical with the vacuum dimensions of the chamber, so that these particles flow directly from the sources of evaporation to the substratum.

2- Cell fabrication

Indium doped tin oxide (ITO, 8 ohm resistant, 83 % transmitted) coated by glass several times washed in an ultrasonic bath with acetone, ethanol, and distilled water to remove impurity, and then dried with a blower of air. The following process was followed by a dye-sensitized solar cell (1,5 * 2 * 0,1 cm):

A colloidal solution of ZnO, CuO, and mixed ZnO-Cu_2O nanostructure was prepared by mixing Nano oxides powder with ethanol. The photoanode was obtained using a dropper to cover colloid solution on the conductive side of the glass and then annealed at 200 °C for 30 min in air. After being cooled, the oxides nanostructure electrode was immersed into 0.05 M Cu (II) complexes azo ligand for 3 hours at room temperature. The counter electrode was Aluminum film coated on ITO glass by Vacuum thermal evaporation technique. Sensitized oxides nanostructure (photoanode) and the Aluminum film-coated (counter electrode) were assembled

the liquid electrolyte (I^-/I^{-3}) solution Fall through capillary action penetrated the workspace, the cell was retained with the binder clip [12].

3. Results and discussions

3.1.1 XRD characterization of oxides

The nanocomposite structure (zinc oxide-copper oxide) were investigated by x-ray diffraction type (SHIMADZU XRD-6000). The XRD using CuKα radiation line of 1.54 A˚ wavelength in 2θ with range 10˚- 80˚.

The XRD patterns of the ZnO powder are shown in Figure (1), it is cleared that powder has a Hexagonal structure, according to ASTM (American Society for Testing and Materials) card No. (00-36-1451) without any impurity as compared with data obtained in the literature [24,25]. That the diffraction peaks were brooding with different intensity, the 2Θ (deg) for ZnO 0.02 M at 400 ˚ C, appeared in 31.63 ˚, 34.65 ˚, 36.16˚, 47.84 ˚, 56.70 ˚, 62.75 ˚, 66.13 ˚, 67. 03˚, 69.12 ˚, 72.74 ˚, and 77. ˚ corresponding reflecting planes are (100), (002), (101), (102), (110), (103), (200), (112) ,(201), (004)and (202) respectively the average crystal size ZnO was 18.36 nm with FWHM 0.696 at 2 θ = 36.26 .

The XRD of CuO patterns shows that each of the diffraction peaks is in perfect alignment with the standard CuO diffraction information (JCPDS NO.48-1548), no characteristic peaks have been found for other oxides. The 2Θ (deg) of CuO can be seen in figure (1). The diffraction peaks for 0.02 M exhibition a most brooding pattern at 32.38 ˚, 35. 58 ˚, 38. 81 ˚, 48.79 ˚, 58.85 ˚, 61.23 ˚, 66.13 ˚ and 67.21 ˚ corresponding reflecting planes are (110), (002), (200), (20^-2), (202) (11^-3), (31^-1) and (113) respectively.

The XRD pattern (MIX) showed a new phase of cubic Cu_2O Copper(I) oxide Figure(1) the diffraction peaks at (2θ) = 31.77 ˚, 34.37 ˚, 36.22 ˚,56.77 ˚, and 72.62 ˚ correspond to the reflection from (100), (002), (101),(110) and (004) ZnO crystal planes and that is in good agreement with hexagonal wurtzite ZnO structure (JCPDS NO.36-1451). While the peak at 39.56 ˚,47.78 ˚,53.39˚,62.97˚and 67.88˚ are due to reflection from (200),(221),(211),(220)and (221) plane are in perfect alignment with those taken from the standard diffraction results for cubic Cu_2O (JCPDS NO.34-1351).

Besides, the sample average crystallite sizes (D) were calculated by using Debye-Scherer equation [26]:

$$D = \frac{K\lambda}{B\ COS\theta} \text{ ----------equation (1)}$$

Where, K = constant equal to 0.9, λ = wavelength of Cu Kα radiation,(*B*) = (FWHM) = Full width half maximum of the diffraction peak expressed in theta then converted to radians and θ = Bragg angles of the principal planes.

The average crystal size is 18.36, 13.12, 16.55 nm for ZnO with hexagonal wurtzite, CuO with monoclinic and ZnO-Cu_2O Link within the crystal lattice. The significant shifts in the XRD mixed pattern suggest that the alteration of the ZnO with the CuO will change the structure of

the ZnO. The crystalline size is reduced due to the lattice distortion caused by the radius difference between both the Zn and Cu ions. The different radii size causes a strain field or stress that disrupts the process of grain growth. The ionic radius of Cu^{2+} is smaller than that of Zn2 +, and the ionic space is smaller; the agglomeration is more likely. Thus, being smaller, Cu^{2+} shows a greater tendency towards agglomeration than Zn^{2+}. In mixed with 0.5:0.5 M, the chances of agglomeration decreasing as the concentration of Cu^{2+} ions increases [27].

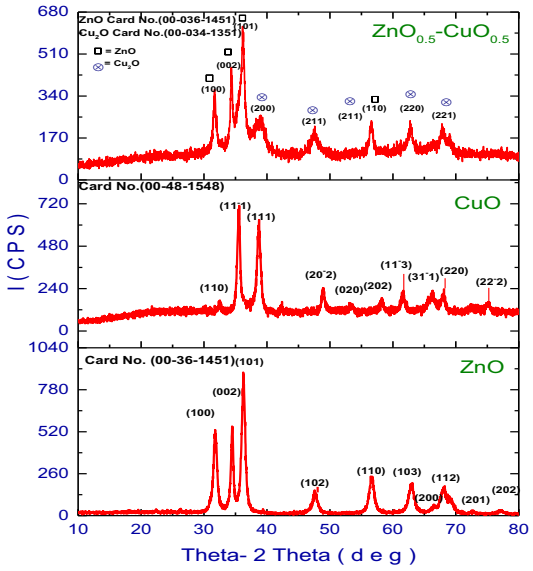

Figure (1) The XRD pattern of ZnO,CuO and ZnO-CuO

3.1.2 XRD characterization of nano copper complexes

The X-ray powder diffraction pattern for nano Cu (II) complex, the metal complex displayed a certain amount of well defined broad crystalline peaks, which proved that these complexes were small crystalline nano size as presented in Figure (2)

Also, the sample average crystallite sizes (D) were calculated by using the Debye-Scherer Equation (1), The average size of crystallites Estimated by applying the Debye-Scherer equation was about (7.084) nm

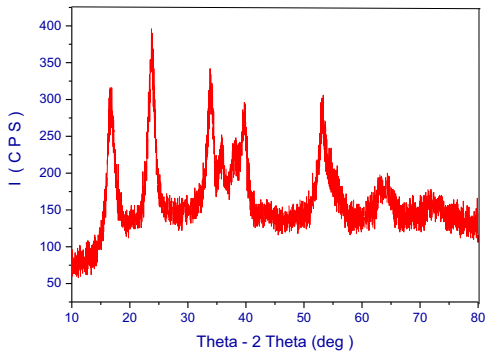

Figure (2) XRD pattern of nano Cu (II) complex

3.2.1 SEM characterization

The morphology of synthesized powders was investigated using scanning electron microscopy (SEM) images of zinc, copper, and znO0.5-Cu2O0.5 nanostructure, illustrating CuO 's influence on ZnO. The ZnO powder SEM image is shown in figure 3(a) as a partition, whereas the CuO SEM as Mixing Pallets is shown in figure 3(b). The single homogeneous ZnO process with a narrow distribution is authenticated in figure 3(a). These pictures reveal that the synthesized samples have nanoparticle nature and morphology, as reported by [27-28],

The SEM in ZnO0.5-Cu2O0.5 appears in Fig 3(c) as Flakes, and the grain in SEM was 24,17 and 22 nm. The nanoparticles are observed form.

SEM images align with the particle dimensions determined from the formula Debye-Scherrer. Such photos thus support the formation of nanostructure flakes ZnO, CuO, and ZnO0.5-Cu2O0.5.

The EDS technique demonstrates the elemental composition of the analyzed volume with the detection of radios emitted by a bombardment of an electron beam from the material. The X-ray Energy Sparsis (EDS) for ZnO and CuO at 1:1 molar ratio, and the polycrystalline one for ZnO0.5-Cu2O0.

EDS displayed well established peaks that demonstrated the pure form of the synthesized nanomaterials without any other impurity elements or phases as shown in the table (1)

The EDX uses the atomic mass of each measured element. The number of atoms per component was calculated using the atomic percentage at that weight percentage, divided by the total number of atoms per sample multiplied by 100.

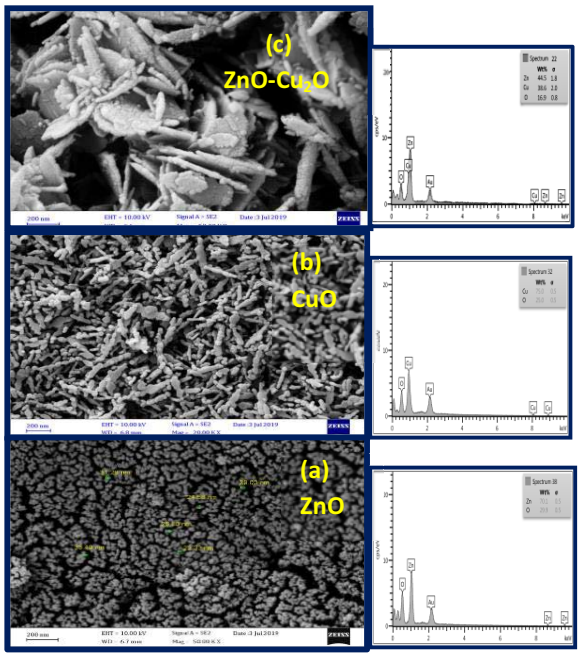

Figure (3) SEM of ZnO, CuO, and ZnO-CuO nanostructure

So do so with all the elements in the sample, for a list of atomic proportions. Sum these together to obtain a total atomic weight. Then for each element in the example, divide its atomic percentage by the total * 100.

So for ZnO theoretical calculate, Zn % =80.347% and for O% =19.652 %, so total percentage 80.348%, +19.652% =100%, While (EDX) for CuO theoretical calculate,Cu % = 79.89% and for O% = 20.11 %, so total percentage 79.89 % + 20.11 % =100%,

So for ZnO-CuO theoretically calculate,
Cu % = 39.47% , Zn % =40.638%
And for 2O% = 19.88 %, so total percentage 39.47 % +40.63 % + 19.88 %=100%
While the practical value from EDX in a table (1)

Table (1) illustrates the average particle size (nm), Shape, and practical EDX.

Sample	Average Particle size(nm)	Particle shape	practical EDX		
			Zn%	Cu%	O%
ZnO	24	Particle	70.1	---	29.9

CuO	17	Merging pallets	---	75.0	25.0
ZnO-Cu_2O	22	Flakes	44.5	38.6	16.9

3.2.2 SEM of Nano copper complexes

the SEM image analysis of the complex as can see in figure (4) having The fibers shape with a percent of spherical Shape with an average size of 20 nm, and the presence of two forms due to the formation of the cis and trance of the nanostructure [28].

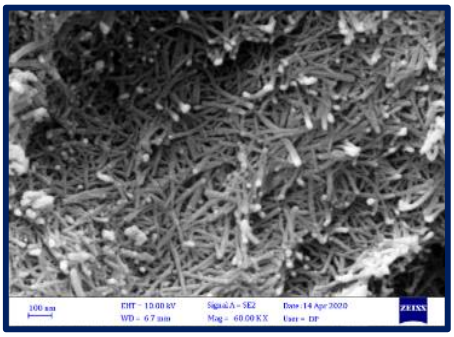

Figure (4) SEM of Nano copper complex

3.3 AFM

Surface morphology was represented using atomic force microscopy (model AA3000, Angstrom Advanced Inc., USA). The 3D image figures (5) (a) illustrate that image as a particle with high vertical order and different form surface homogeneity and (b) Granularity accumulation distribution chart of the ZnO CuO and mixed nanostructure, illustrate that the difference inhomogeneity of the surface with mixed oxide, the lowest and highest value of the granular volume was ranging from (18-50), (17-40) and (20-55) nm .with the most significant proportion of the distribution of nanoparticles was <=90% Diameter:24, 23and 33 nm, The average grain size was 25.36, 26.72 and 36.10 nm for (Zn, Cuo and Zn -Cu_2O) respectively.

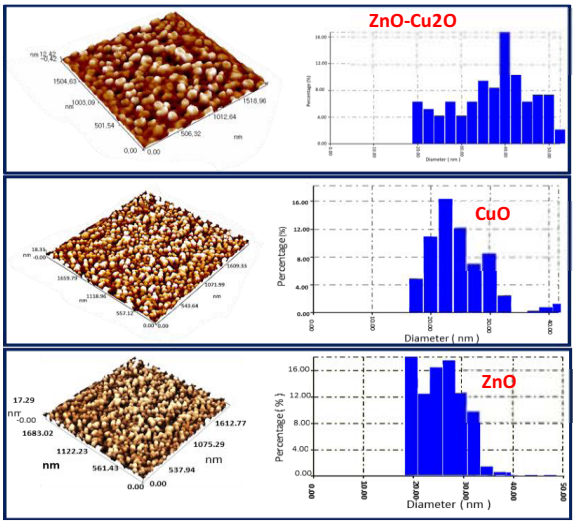

Figure (5) AFM of ZnO, CuO, and ZnO-CuO nanostructure

While the AFM of Nano copper complex Nano complex has a hemispherical shape with perfect symmetric granules and vertically aligned, the estimated values of grain size were 20.12 nm, and the root means square of the surface was 0.763 nm, and roughness was 0.632 nm. The 3dimension atomic force microscopy images and granularity growth distribution chart of the Nano complex are shown in Figure (6).

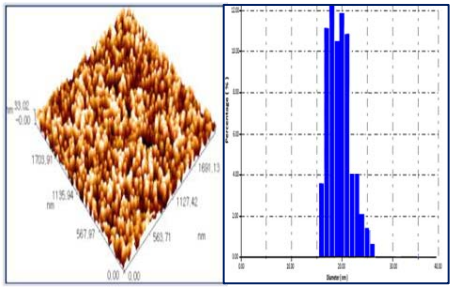

Figure (6) AFM of Nano copper complex

3.4 UV-VIS

(UV-Vis) spectrophotometer model Shimadzu UV-Vis 160V were measured from 200-900 nm, using 1.0 cm length quartz cells. UV-vis absorption spectra of ZnO, CuO, and ZnO0.5 - $CuO_{0.5}$ oxides nanostructure are obtained from the figure (7), λ max = 340.98 nm The absorption of CuO is found to have been slightly shifted to a longer wavelength (redshift) with λ max = 857.48 nm as compared with ZnO absorption spectrum due to S, a p-d spin exchange between both the delocalized s-or p-type band electrons of Cu and O atom [29]. While λ max for mixed showed absorption spectrum at λ max = 413.44 nm.

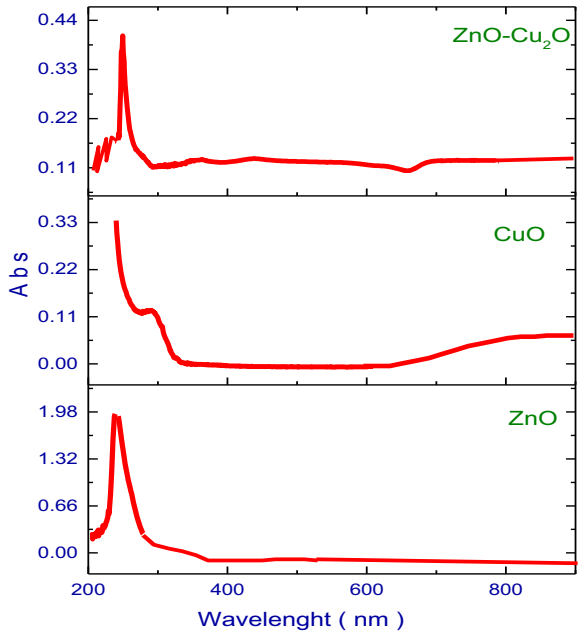

Figure (7) UV-vis absorption spectra of ZnO, CuO, and $ZnO_{0.5}$ - $CuO_{0.5}$

From Uv –Vis data the Bandgap energy " Eg " (ev) calculate by taut plots [30] as shown in figure (8) By extrapolating the linear part of the curve gave (Eg)as (3.63,1.54 and 2.94)eV for ZnO, CuO, and $ZnO_{0.5}$ - $CuO_{0.5}$ oxides respectively. The energy gap of nanomaterials changes as the size of crystal changes(18).

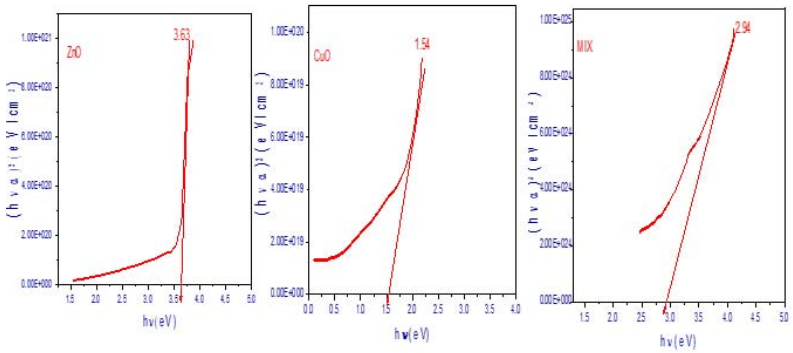

Figure (8) the Bandgap energy " Eg " (ev)from taut plots.

3.5 The Dye-sensitized solar cells parameters

The cells parameters as shown in figures (9)-(11); Isc, Voc, Imax, and Vmax were estimated from the below I-V curves, while the fill factor (ff) and the cell efficiency were calculated using the equations [12]:

$$\eta = \frac{P_m}{P_{in}} x100\% = \frac{I_m V_m}{P_{in}} x100\% \quad \text{--------- equation (2)}$$

$$F.F = \frac{J_m V_m}{J_{sc} V_{oc}} \quad \text{--------- equation (3)}$$

All measurements are tabulated in the table (2)

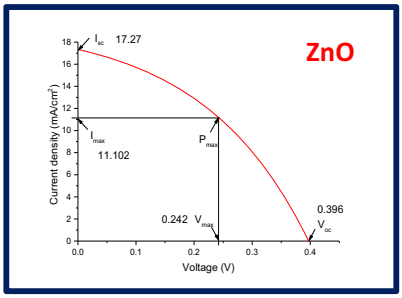

Figure (9) photovoltaic properties of the DSSC for ZnO

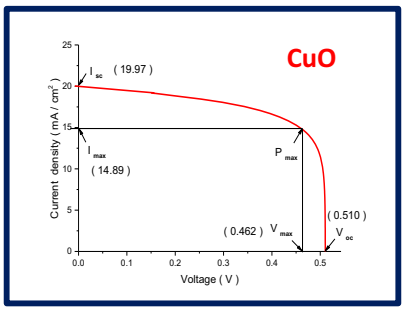

Figure (10) photovoltaic properties of the DSSC for CuO

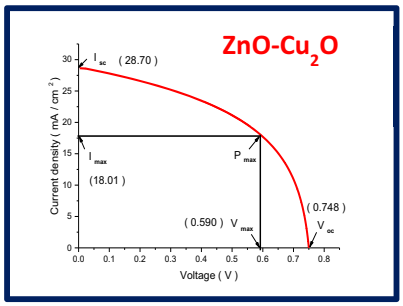

Figure (11) photovoltaic properties of the DSSC for ZnO-Cu_2O

Table (2) illustrate the cells parameters of ZnO,CuO and mixed

DSSC	Voc (V)	J sc (A/cm^2)	V_{max} (V)	J_{max} (A/cm^2)	P_{max} (W/cm^2)	FF	η %
ZnO	0.396	0.017	0.24	0.011	0.0026	0.392	2.67
CuO	0.510	0.019	0.46	0.014	0.0067	0.675	6.8
MIX	0.748	0.028	0.59	0.018	0.0106	0.494	10.62

Conclusion

A systematic study of ZnO with hexagonal wurtzite, CuO with monoclinic and ZnO-Cu_2O Link within the crystal lattice was successfully synthesized using the photo-irradiation method. Crystallites size from X-ray diffraction shows (18.36, 13.12, and 16.55) nm. The average grain size from the AFM shows (25.36, 26.72, and 36.10 nm for (Zn, Cuo, and Zn -Cu_2O), respectively. In this study. It has been observed that the ZnO-Cu_2O nanostructure has the excellent conversion efficiency (PCE) as compared with ZnO and CuO only, the nano dye used

to develop the dye-sensitized solar cells, by replacing the traditional organic dyes with azo nano copper complex.

References: -

1. Hayat MB, Ali D, Monyake KC, Alagha L, Ahmed N. Solar energy—A look into power generation, challenges, and a solar-powered future. Int J Energy Res. 2019;43(3):1049–67.
2. Li GR, Gao XP. Low-Cost Counter-Electrode Materials for Dye-Sensitized and Perovskite Solar Cells. Adv Mater. 2020;32(3):1–20.
3. Unni GE, Vineeth. Photovoltaic Application of Rice Flake-Shaped ZnO Nanostructures. Electron Mater. 2020;
4. Zhang W, Chang S, Yao S, Wang H. Preparation and Characterization of Submicron Star-Like ZnO as Light Scattering Centers for Combination with ZnO Nanoparticles for Dye-Sensitized Solar Cells. J Electron Mater. 2019;48(8):4895–901.
5. Kilic B. Produce of carbon nanotube/ZnO nanowires hybrid photoelectrode for efficient dye-sensitized solar cells. J Mater Sci Mater Electron [Internet]. 2019;30(4):3482–7. Available from: http://dx.doi.org/10.1007/s10854-018-00624-y
6. Rheima AM, Mohammed MA, Jaber SH, Hameed SA. Synthesis of Silver Nanoparticles Using the UV-Irradiation Technique in an Antibacterial Application. Journal of Southwest Jiaotong University. 2019;54(5).
7. Mohammed MA, Rheima AM, Jaber SH, Hameed SA. The removal of zinc ions from their aqueous solutions by Cr2O3 nanoparticles synthesized via the UV-irradiation method. Egyptian Journal of Chemistry. 2020 Feb 1;63(2):5-6.
8. Rheima AM, Mohammed MA, Jaber SH, Hasan MH. Inhibition effect of silver-calcium nanocomposite on alanine transaminase enzyme activity in human serum of Iraqi patients with chronic liver disease. Drug Invention Today. 2019 Nov 15;12(11).
9. Rheima, A.M., D.H. Hussain, and H.I. Abdulah, *Silver nanoparticles : Synthesis, Characterization and their used a counter electrodes in novel Dye sensitizer solar cell.* IOSR Journal of Applied Chemistry, 2016. **9**(10): p. 6–9.
10 Hussain DH, Rheima AM, Jaber SH, Kadhim MM. Cadmium ions pollution treatments in aqueous solution using electrochemically synthesized gamma aluminum oxide nanoparticles with DFT study. Egyptian Journal of Chemistry. 2020 Feb 1;63(2):417-24
11. Rheima AM, Hussain DH, Almijbilee MM. Graphene-Silver Nanocomposite: Synthesis,

and Adsorption Study of Cibacron Blue Dye from Their Aqueous Solution. Journal of Southwest Jiaotong University. 2019;54(6).

12. Hussain DH, Abdulah HI, Rheima AM. Synthesis and Characterization of ɣ-Fe2O3 Nanoparticles Photo Anode by Novel Method for Dye Sensitized Solar Cell. International Journal of Scientific and Research Publications. 2016;6(10):26-31.
13. Jabber SH, Hussain DH, Rheima AM, Faraj M. Comparing study of CuO synthesized by biological and electrochemical methods for biological activity. Al-Mustansiriyah Journal of Science. 2019;30(1):94-8.
14. Ismail AH, Al-Bairmani HK, Abbas ZS, Rheima AM. Synthesis, characterization, spectroscopic, and biological activity studies of Nano scale Zn(II), Mn (II) and Fe (II) theophylline complexes. Journal of Xi'an University of Architecture & Technology. 2020; XII (II): 2775-2789.
15. Ali AA, Al-Hassani RM, Hussain DH, Rheima AM, Abd AN, Meteab HS. Fabrication of Solar Cells Using Novel Micro-and Nano-Complexes of Triazole Schiff Base Derivatives. Journal of Southwest Jiaotong University. 2019;54(6).
16. Ali AA, Al-Hassani RM, Hussain DH, Rheima AM, Meteab HS. Synthesis, spectroscopic, characterization, pharmacological evaluation, and cytotoxicity assays of novel nano and micro scale of copper (II) complexes against human breast cancer cells. Drug Invention Today. 2020; 14(1).
17. Ismail AH, Al-Bairmani HK, Abbas ZS, Rheima AM. Nanoscale Synthesis of Metal (II) Theophylline Complexes and Assessment of Their Biological Activity. Nano Biomed. Eng. 2020;12(2):139-47
18. Abdulah HI, Hussain DH, Rheima AM. Synthesis of α-Fe2O3, γ-Fe2O3 and Fe3O4 Nanoparticles by Electrochemical Method. Journal of Chemical, Biological and Physical Sciences 6(4):1288-1296
19. Li Q, Wang Q, Chen Z, Ma Q, An M. A facile and flexible approach for large-scale fabrication of ZnO nanowire film and its photocatalytic applications. Nanomaterials. 2019;9(6).
20. Luo J, Wang Y, Zhang Q. Progress in perovskite solar cells based on ZnO nanostructures. Sol Energy [Internet]. 2018;163(January):289–306. Available from: https://doi.org/10.1016/j.solener.2018.01.035

21. Waghadkar Y, Chauhan R. Highly efficient dye-sensitized solar cells by TiCl4 surface modification of ZnO nano-flower thin film. J Solid State Electrochem. 2018;22(11):3621–30.
22. Moritz M, Geszke-Moritz M. The newest achievements in synthesis, immobilization and practical applications of antibacterial nanoparticles. Chem Eng J. 2013;228:596–613.
23. Qiu S, Zhou H, Shen Z, Hao L, Chen H, Zhou X. Synthesis, characterization, and comparison of antibacterial effects and elucidating the mechanism of ZnO, CuO and CuZnO nanoparticles supported on mesoporous silica SBA-3. RSC Adv. 2020;10(5):2767–85.
24. Katayama J, Ito K, Matsuoka M, Tamaki J. Performance of Cu2O/ZnO solar cell prepared by two-step electrodeposition. J Appl Electrochem. 2004;34(7):687–92.
25. Guo S, Hayakawa K, Link C. (Article begins on next page). Diabetes. 2016;60(8):1789–96.
26. Muniz FTL, Miranda MAR, Morilla Dos Santos C, Sasaki JM. The Scherrer equation and the dynamical theory of X-ray diffraction. Acta Crystallogr Sect A Found Adv. 2016;72(3):385–90.
27. Mahajan P, Singh A, Arya S. Improved performance of solution processed organic solar cells with an additive layer of sol-gel synthesized ZnO/CuO core/shell nanoparticles. J Alloys Compd [Internet]. 2020;814:152292. Available from: https://doi.org/10.1016/j.jallcom.2019.152292
28. Saravanan P, SenthilKannan K, Divya R. A perspective approach towards appreciable size and cost-effective solar cell fabrication by synthesizing ZnO nanoparticles from Azadirachta indica leaves extract using domestic microwave oven. J Mater Sci Mater Electron [Internet]. 2020;31(5):4301–9. Available from: https://doi.org/10.1007/s10854-020-02985-9
29. Song J. Colloidal metal oxides in electronics and optoelectronics [Internet]. Colloidal Metal Oxide Nanoparticles. Elsevier Inc.; 2020. 203–246 p. Available from: http://dx.doi.org/10.1016/B978-0-12-813357-6.00011-5
30. Viezbicke BD, Patel S, Davis BE, Birnie DP. Evaluation of the Tauc method for optical absorption edge determination: ZnO thin films as a model system. Phys Status Solidi Basic Res. 2015;252(8):1700–10.